

# Simple maps with periodic parameter fluctuations: a source for complex periodic motion which is indistinguishable from chaos

L. Hector Juárez<sup>1</sup>, Holger Kantz<sup>2</sup>, Oscar Martínez<sup>2</sup>, Eduardo Ramos<sup>3</sup> and Raul Rechtman<sup>3</sup>

<sup>1</sup>Departamento de Matemáticas, Universidad Autónoma Metropolitana (Iztapalapa, Apdo. Postal 55-534, 09340 México D.F., México,

<sup>2</sup>Max-Planck-Institut für Physik komplexer Systeme, Nothnitzer Str. 38, D-01187 Dresden, Germany

<sup>3</sup>Centro de Investigación en Energía, Universidad Nacional Autónoma de México, Apdo. Postal 34, 62580 Temixco, Mor., México

(Dated: November 27, 2018)

We study systems with periodically oscillating parameters, which introduce transitions from chaotic to periodic behavior and vice versa. Performing the long time limit, we can define ergodic averages such as Lyapunov exponents, where a negative maximal Lyapunov exponent corresponds to a stable periodic orbit. By this, extremely complicated periodic orbits composed of laminar phases and chaotic bursts appear in a very natural way. When a tiny amount of noise is coupled to the system, dynamics with positive and with negative maximal Lyapunov exponents are indistinguishable. We discuss two physical systems, an oscillatory flow inside a duct and a dripping faucet with variable water supply, where such a mechanism seems to be responsible for a complicated alternation of laminar and turbulent phases.

PACS numbers: 05.45.Ac, 47.60.+i

## I. INTRODUCTION

Seasonal variations are a prominent source of slow periodic parameter fluctuations in biological, ecological, geochemical and geophysical systems. But also in many technical and physical situations, slow periodic oscillations of system parameters do occur. Speaking of time dependent parameters, we imply that there is no feedback from the system under study onto the variation of the parameters, whose time dependence can either be considered as been given (non-autonomous situation) or can be ruled by its own periodic autonomous dynamics. Moreover, we focus on situations where the typical time scales related to the system dynamics for fixed parameters is much faster than the time scale related to the parameter variation, as it is typical of many processes subject to seasonal variations. The opposite case, where both time scales are comparable has been studied as an open loop control mechanism [1, 2].

In what follows we discuss a scenario, where slow parameter fluctuations introduce transitions from chaos to periodic behavior and back, so that the motion in the long run is an alternation between these two types of behavior. We will show that ergodic averages can be performed as usual and hence the motion in the long time limit is clearly classified to be either periodic or chaotic. However, as our analysis will show, in practical applications, an overall chaotic motion will be indistinguishable from an overall periodic motion, both in numerical simulations and in experiments. In the latter case, this is another example of "stable chaos" [3]. This indistinguishability implies a robustness of the phenomenon despite that fact that there are parameter regimes where stable periodic motion and chaos are both supported by a dense set of parameters.

This rather unexpected behavior is shown to exist in numerical experiments of an oscillating flow inside a duct and a dripping faucet with variable liquid supply.

## II. MAP WITH PERIODIC PARAMETER VARIATIONS

Many physical experiments and the corresponding model systems possess solutions which, due to dissipation, relax to rather uninteresting fixed points. Such systems are often exposed to a periodic driving, such as electric resonance circuits. In particular when the system without driving has a two-dimensional phase space, chaos can only appear with the driving term.

This paper deals with a very different class of driven systems; we assume that our system without driving can behave chaotically, depending on the values of a control parameter. This parameter is then varied periodically, with a period which is much longer than the time scale of the internal dynamics on which the auto-correlation function in the chaotic regime would relax, or which would govern the relaxation to a stable fixed point in parameter regimes where it exists. Hence, the temporal dependence of the control parameter has no influence on the short time dynamics of the system, but it causes transitions between different dynamical behaviors which might exist for different values of the control parameter.

In what follows we choose the quartic map f given by

$$x_{n+1} = f(a; x_n) = 4ax_n(1 - x_n)[1 - ax_n(1 - x_n)] \quad (1)$$

with  $0 < a \leq 4$ . This map has the interesting property that for  $a = a_c = 3.375$  a tangent bifurcation occurs where out of a chaotic region that covers the whole  $[0; 1]$  interval a period one window appears. However, other

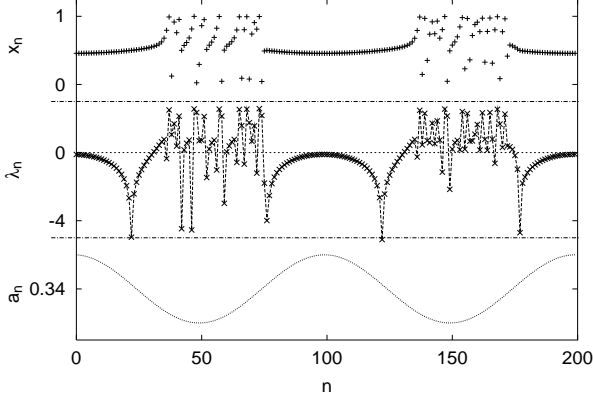


FIG. 1: Two hundred iterates of the map Eq. (2) for  $a_0 = 3.375$ ,  $a_1 = 0.1$ ,  $\ell = 2 \Rightarrow 100$  (top panel), the instantaneous stretching rates  $\ln |f'(a_n; x_n)|$  (middle panel) and the parameter  $a_n$  (bottom panel).

maps can be also be considered, for example the logistic map for values of the control parameter near a period 3 window.

Imposing a temporal dependence on the control parameter leads us to consider the two dimensional skew autonomous system

$$\begin{aligned} n+1 &= n + \ell \\ x_{n+1} &= f(a(n); x_n) \end{aligned} \quad (2)$$

$$= 4a(n)x_n(1-x_n) [1 - a(n)x_n(1-x_n)]$$

where  $a(n) = a_0 + a_1 \cos n$ ,  $a_0$  is chosen near  $a_c$ ,  $a_1 \ll 1$  and  $\ell = 2 \Rightarrow N$ ,  $N \gg 1$ . A small value of  $\ell$  leads to a well defined time scale separation between the parameter variation and the dynamics of the system while the choice of  $a_0$  and  $a_1$  ensure that the system crosses from a chaotic regime to a non chaotic one.

A typical sequence of iterates of Eq. (2) (after discarding a transient) is shown in Fig. 1. We see an alternation between irregular fluctuations of  $x$  and regular episodes. Due to the slowness of the change of  $a$ , the trajectory can relax toward the stable fixed point for those values of  $a_n$  where it exists, whereas it follows a chaotic trajectory for  $a_n > 3.375$ , where the map of Eq. (1) is chaotic.

Since the  $x$ -dynamics is not mixing, this system clearly has (at least) one invariant measure in its two-dimensional phase space for every  $a_0$ , on which ergodic averages are well defined. In particular, every invariant set has two associated Lyapunov exponents. The Jacobian of Eq. (2) reads

$$J_n = \begin{pmatrix} 0 & 1 & 0 \\ a \sin n & \frac{\partial f(a(n); x_n)}{\partial a} & \frac{\partial f(a(n); x_n)}{\partial x_n} \end{pmatrix} A$$

One Lyapunov exponent (corresponding to the  $x$ -dynamics) is zero, whereas the other is found through an average over the invariant measure or over an infinitely

long trajectory, assuming ergodicity. As a consequence, the seemingly intermittent dynamics shown in Fig. 1 has a well defined non-trivial Lyapunov exponent, which can be either positive or negative (or zero). Notice that this alternation between chaotic and regular phases is different from the typical intermittency scenarios [4]. The durations of both the regular and the chaotic phases are related to the relative time intervals the parameter  $a(n)$  is in the chaotic or the periodic regime of the map, respectively and these may be tuned by slight changes of  $a_0$ .

### III. INDISTINGUISHABILITY BETWEEN CHAOTIC AND NON CHAOTIC ORBITS

In the example, Fig. 1, we have chosen  $a_1$  and  $a_0$  such that  $a(n)$  fluctuates around the tangent bifurcation taking place at  $a_c = 3.375$ , where a stable fixed point is born. For fixed  $a > a_c$ ,  $\forall a \in [a_c, 1]$ , any initial condition, after a chaotic transient, settles down on a fixed point  $\hat{x}(a)$ . For fixed  $a < a_c$ ,  $\forall a \in [0, 1]$ , the invariant set is one-dimensional for a dense set of parameter values, but shows type-I intermittency because of the closeness to the tangent bifurcations. Due to the triangular structure of the Jacobian, the maximum Lyapunov exponent (corresponding to the  $x$ -dynamics) is given by  $\lambda_x = \lim_{N \rightarrow \infty} \frac{1}{N} \sum_{n=0}^{N-1} \ln |f'(a(n); x_n)|$ , where the average  $\lim_{N \rightarrow \infty} \frac{1}{N} \sum_{n=0}^{N-1}$  is with respect to the invariant measure under consideration or over an infinitely long trajectory, assuming ergodicity. During one period of the auxiliary variable  $n$ , the parameter  $a(n)$  alternates between the periodic and chaotic regime of the map and therefore  $\lambda_x$  has contributions with negative and positive signs. Depending on which contribution has a larger modulus, the overall dynamics is either chaotic or not. This in turn, depends on the values of  $a_0$ ,  $a_1$  and  $\ell$ .

During the iterates where the trajectory relaxes toward the fixed point  $\hat{x}(a)$ , the tangent space dynamics is contracting, and we call the accumulated contraction factor  $f_c$ . During the iterations when the trajectory looks irregular, its tangent space dynamics is essentially expanding, and we call the accumulated expansion factor  $f_e$ . Then, roughly, the Lyapunov exponent is  $\lambda_x \approx \lim_{N \rightarrow \infty} \frac{1}{N} \sum_{n=0}^{N-1} \ln |f'_n|$ , where  $\lim_{N \rightarrow \infty} \frac{1}{N} \sum_{n=0}^{N-1}$  now denotes the average over successive periods of  $n$ . If we start two trajectories with a distance  $\delta$  at the beginning of the irregular phase, at its end their distance is  $f_e \delta$ . This distance will shrink during the regular phase, and at its end will be  $f_e f_c \delta$ . Hence, if  $f_e f_c$  on average is smaller than unity, two trajectories will approach each other, and finally will be indistinguishable. The stable orbit to which they are attracted is close to the locations of  $\hat{x}(a)$  when  $a > a_c$ , and is an irregular orbit evolving from  $x$  being close to the  $\hat{x}(a)$ , when the parameter is tuned to  $a < a_c$ .

This alternation between contracting and expanding episodes is clearly visible in Fig. 1. A stable periodic orbit thus is as irregular as a chaotic solution, but its

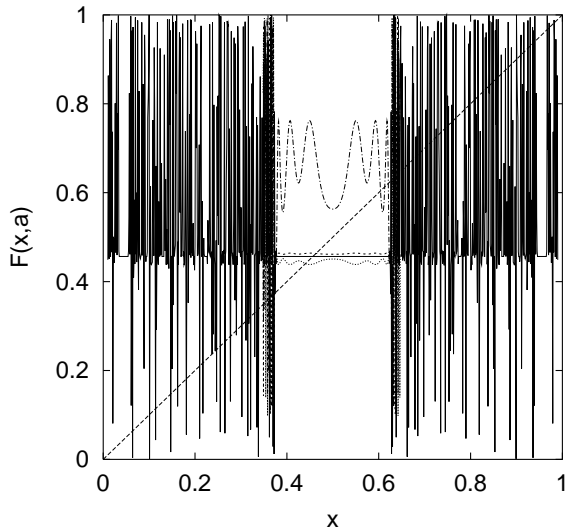


FIG. 2: The full graph  $F(x)$  as defined in the text for  $a_0 = 3.4$ , and the central parts of the graphs of  $F(x)$  for  $a_0 = 3.401, 3.4015, 3.4018$ , respectively (broken lines from bottom to top), showing the birth of the fixed point through a sequence of tangent bifurcations.

irregular segment repeats itself exactly in every period of oscillation of the parameter  $a$ , whereas for a trajectory with a positive Lyapunov exponent it does not. Hence, this system can create arbitrarily complicated periodic orbits, since by the choice of  $N$  one can determine the period length and also, how many points of the periodic orbit are in the irregular regime. When the  $n$ -dynamics is quasi-periodic instead of periodic (by choosing  $N$  as an irrational number), also orbits with negative Lyapunov exponent have non-repeating irregular segments. By visual inspection, these cannot be distinguished from orbits with a positive Lyapunov exponent.

#### IV. THE STROBOSCOPIC VIEW

The special dynamics of  $n$  hinders the 2-dimensional map of Eq. (2) of having a fixed point. The shortest periodic orbit can have length  $N$  when  $! = 2 \Rightarrow N$ . Therefore, it makes sense to study the composition of  $N$  successive iterates  $F(x) = \prod_{n=1}^N f(a(n); x_n)$ . When the Lyapunov exponent of Eq. (2) is negative,  $F$  should have a stable periodic orbit or fixed point, whereas it has only unstable periodic orbits and chaotic solutions for positive exponents. In Fig. 2 we show the graph of  $F$  for several values of  $a_0$ . Around  $a = 3.375$ ,  $F(x)$  has an almost super-stable fixed point. These fixed points are generically born and eliminated by tangent bifurcations, together with their unstable counterparts. For every initial phase  $\phi_0$  we have a different stroboscopic map  $F(x)$ . However they are all topologically conjugate. For our choice of the variation of  $a(n)$ , however, the existence or absence of a stable fixed point can best be seen when

$\phi_0 = 0$ , where each orbit of the system Eq. (2) assumes values close to the fixed point of  $f(x; a)$  in Eq. (1) for fixed  $a = a_0 + a_1$ .

#### V. NOISE AND ROUND-OFF EFFECTS

The results described above, and in particular the distinction between motion corresponding to negative and positive Lyapunov exponents, is correct only in the abstract mathematical setting. On a computer, the finite precision of the internal representation of real numbers can enforce the motion onto a complex periodic orbit although its Lyapunov exponent is positive. This happens, when the accumulated contraction  $f_c$  during the laminar phase is too strong, so that at the end of this phase the trajectory has no memory of the turbulent or chaotic phase. The contraction factor  $f_c$  is the average of the instantaneous stretching rates  $\ln |f'(a_n; x_n)|$  on the laminar phase. For typical values of  $a_0$  and  $a_1$  we found numerically that orbits with a positive Lyapunov exponent became periodic when the laminar phase contained more than thirty iterates. If the laminar phases are shorter, either because the period  $N$  is small enough, or because  $a_0$  is chosen to be inside the chaotic regime, orbits with positive Lyapunov exponents are non-periodic as expected. Hence, with finite precision and large  $N$ , one cannot decide, without computation of the Lyapunov exponent, whether the system has a stable periodic orbit or not.

In an experimental realization, instead of computer round-off errors there is external noise coupled into the system. Equation (1) has then to be modified by adding white noise  $\eta_n$ , where  $0 < \eta_n \leq 1$ ,  $h_{n,n+1} = \eta_n$  and  $h_{n,n} = 0$ . This has no visible effect on chaotic solutions of Eq. (2), but it does destroy the periodicity of stable periodic solutions. Inside the expanding and hence irregular sections, noise is exponentially amplified and creates orbits which appear chaotic. Systems like Eq. (2) therefore have periodic orbits which are extremely sensitive to external noise, despite linear stability.

#### VI. PARAMETER DEPENDENCE

The rather complex sequence of tangent bifurcations leading to the creation and destruction of the stable periodic orbits causes the orbits to depend sensitively on the system parameters, so that there is a complicated hopping from periodic to chaotic motion as a function of every single control parameter such as  $a_0, a_1$ , or  $N$  in our example, as illustrated in Figs. 3-5. In the first one, we show the Lyapunov exponent  $\lambda$  as a function of  $a_0$  ( $a_1$  and  $N$  fixed) and note that the change from chaotic to stable periodic solutions is very complicated, leading us to assume that both types of behaviors are supported by a dense set of parameters. The same conclusion follows from Fig. 4 where we show the Lyapunov diagram for the  $x$ -dynamics [5]. We found the fractal dimension of

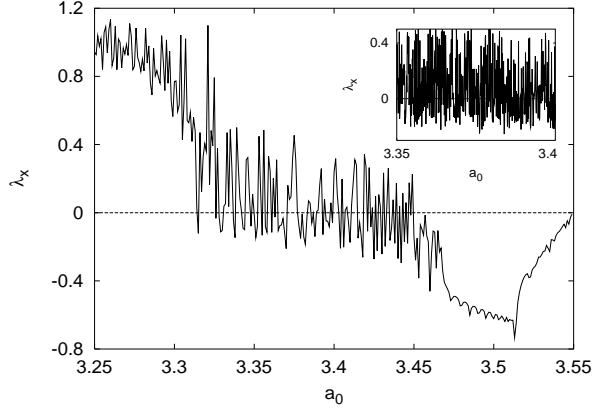


FIG. 3: The Lyapunov exponent of the x-dynamics,  $\lambda_x$ , as a function of the parameter  $a_0$  for the system Eq. (2) ( $a_1 = 0.1$ ,  $\Omega = 2$ ,  $N = 100$ ). The inset shows a smaller interval of the control parameter at a higher resolution.

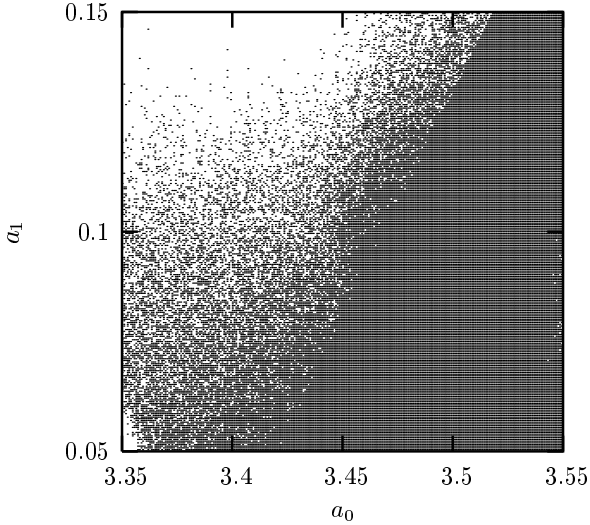


FIG. 4: Lyapunov diagram with  $N = 100$ . Black dots correspond to a negative Lyapunov exponent, white to a positive one. A total of 65,536 dots are drawn.

the boundary between stable and unstable solutions by finding the scaling of the number of {uncertain points} as  $\epsilon$  is varied [6, 7]. A point  $(a_0; a_1)$  is {uncertain} if in a neighborhood of radius  $\epsilon$  there exists at least one point where the Lyapunov exponent has an opposite sign to the one evaluated at  $(a_0; a_1)$ . In Fig. 5 we show those points of the previous figure that are {uncertain} for  $\epsilon = 10^{-7}$ . From the scaling of the number of uncertain points with  $\epsilon$  we found the box counting dimension  $D_0$  of the boundary between chaotic and stable solutions to be  $D_0 = 1.985$ . This result gives a quantitative support to the idea that both stable and unstable orbits have a dense set of parameters. We also found that increasing  $D_0 \rightarrow 2$  for  $N > 100$  and also for  $N < 20$  while it has a minimum value  $D_0 = 1.8$  for  $N = 30$ .

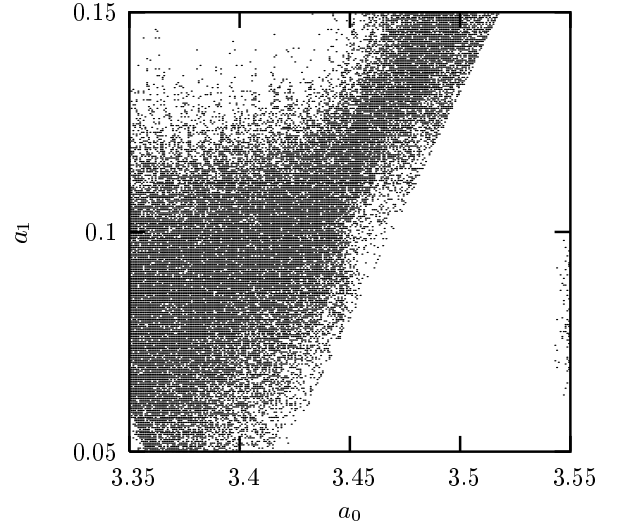


FIG. 5: Black dots represent the {uncertain points} with  $\epsilon = 10^{-7}$ , and  $N = 100$ .

## VII. OSCILLATORY FLOW IN A DUCT

As a first example that displays the behavior discussed previously we briefly present results of numerical experiments of an oscillatory flow in a duct filled with fluid. This flow can be generated by imposing oscillatory pressure or velocity fields at the ends of the duct with suitably defined phase lags. The stability of these flows can be described in terms of two nondimensional parameters, the oscillatory Reynolds number  $R$  and the Stokes parameter  $\beta$ . These are defined by  $R = U \sqrt{\rho/\mu}$  and  $\beta = D/\delta$  where  $U$  is a characteristic velocity,  $\rho$  is the kinematic viscosity of the fluid,  $D$  a characteristic distance of the duct, and  $\delta$  the Stokes penetration depth. This last quantity is defined by  $\delta = \sqrt{2\nu/\omega}$  with  $\omega$  the frequency of the oscillation. It is a well established fact that zones of distinct dynamical qualitative behavior can be identified in the  $(R, \beta)$  space. Specifically, it has been experimentally observed that for  $\beta \leq 2$  and  $R < 500$ , the flow is laminar, while for  $R > 500$ , the flow inside the duct is laminar for the phase intervals where the velocity is small while bursts with a frequency much larger than the forcing appear near the end of the acceleration phase [8]. As  $R$  is increased, the phase interval where high frequency oscillations are present gets larger, but it never covers the cycle entirely. The origin of the high frequency oscillations is the generation of vortices due to the instability of the laminar flow. Numerical results agree with the experiment [9].

In particular, Fig. 6 shows the axial  $u$  and transversal  $v$  velocities in the middle of a duct. As can be observed, when the velocity is close to zero, the trace is smooth, indicating laminar flow, however, high frequency oscillations appear when the velocity reaches its maximum absolute value in each cycle. Taking  $v_{\max} = U/D$ , as the

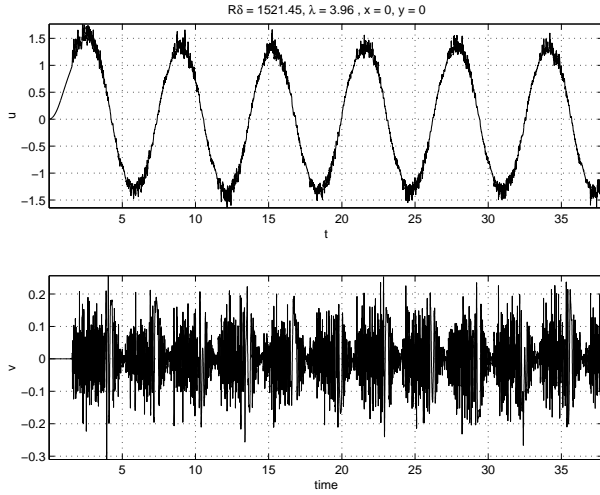


FIG. 6: Time history of axial and transversal velocities at the center of a two dimensional duct with expansions at the ends and with an aspect ratio (total length/cross section) of 20,  $R = 1521$  and  $\lambda = 4$ .

lower limit of the characteristic frequency of the vortices, then the ratio of the vortices frequency to the forcing frequency,  $\omega_v/\omega$  is  $2R =$  which for this example is 768. This indicates that the changes in the driving force are slow compared with the internal vortex dynamics corresponding with the conditions discussed in the previous sections.

### VIII. DRIPPING FAUCET WITH VARIABLE SUPPLY

Our second example describes the dynamics of a dripping faucet with variable liquid supply. This problem, with constant liquid supply has been studied extensively [10]. The time interval  $T$  between successive drops shows a complicated bifurcation diagram as the water supply increases. There are two studies that are important in the context of the present analysis. The model presented by Fuchikami et al [11] is relevant because it is built on sound physical phenomenology, but unfortunately is not simple and long time calculations involving many drops are extremely computing intensive. On the other hand, the model presented by Coulet et al [12] which is based on the former, is useful since it is simple and can be used for exploring the long time behavior. Both models can be adapted to analyze the system when the liquid supply varies as a harmonic function of time and they display a similar behavior with constant and variable liquid supply.

The Coulet model with constant liquid supply has a complicated bifurcation diagram and we choose a value  $\phi_0$  that separates a zone with irregular behavior from a period four window. We now consider a variable liquid supply that varies harmonically around a value near  $\phi_0$

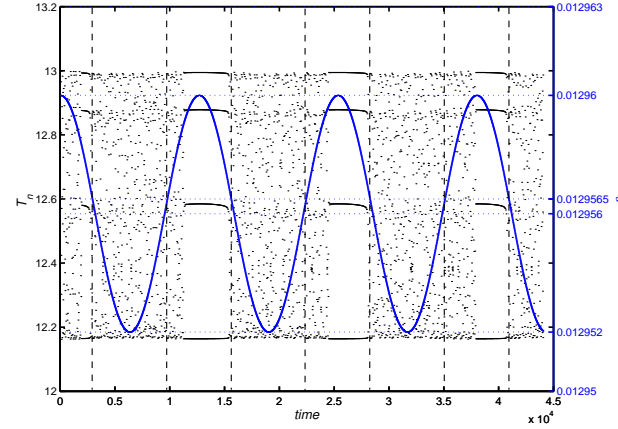


FIG. 7: The dripping faucet with varying liquid supply. Oscillation amplitude =  $4 \times 10^{-6}$ , oscillation period =  $12.66 \times 10^3$ .

with a period which is approximately 1000 times larger than the characteristic period of the subsequent drop release with constant liquid supply and with an amplitude

chosen in a way that the water supply does not extend outside the period four window. These conditions allow the system to visit alternatively a zone of irregular behavior and a zone of period four in the map of constant liquid supply. The result of the periodic variation of the water supply are shown in Fig. 7. The continuous sinusoidal line represents the liquid supply and the dots the values of the time intervals between successive drops. As can be clearly seen, the system presents zones of periodic and chaotic behavior as for the map of Eq. (2).

### IX. CONCLUSIONS

We discussed systems with periodic parameter fluctuations which are driven from regular to chaotic motion and back. Although simple in its construction, this type of dynamics creates very complicated orbits. In computer simulations and in real experiments, it is impossible to distinguish the existence of stable complex periodic solutions and of chaotic solutions in the underlying model, since round-off errors and noise interact with the dynamics.

Our considerations are not restricted to discrete time maps, since the same phenomena are expected to exist for flows as well. It is also not relevant to assume sinusoidal variation of the parameter, so that we expect such a behavior to be rather widespread.

We presented two numerical experiments that illustrate the change of behavior due to a periodic variation of a parameter with a time scale much larger than the natural time scale of the system.

## A cknow ledgm ents

A ssistance of H ector Cortes and A lfredo Q uiroz with num erical calculations is gratefully acknow ledged. This

work has been partially supported by D G A P A {UNAM under G rant No. IN103300.

- 
- [1] K . A . M inus and J . C . Sprott, Phys. Rev. E 59 5313 (1999).
  - [2] R . L in a, M . Pettini, Phys. Rev. A 41 726 (1990).
  - [3] A . P oliti, R . L ivi, G . L . O ppo, R . K apral, Europhys. Lett. 22, 571 (1993).
  - [4] Y . P om eau, M anneville, Comm . M ath. Phys. 74, 189 (1980).
  - [5] M . M arkus, B . H ess, Comput. & Graphics 13 (1989) 553.
  - [6] S . B leher, C . G rebogi, E . O tt, R . B rown, Phys. Rev. A 38 (1988) 930.
  - [7] E . O tt, Chaos in Dynam ical System s, C . U . P ., 1993.
  - [8] M . H ino, M . Sawam oto, and S . Takasu, J. Fluid M ech. 75 193-207 (1976).
  - [9] L . H . Juarez and E . Ram os, Com pt. Rend A cad. Scien. Fr., 331, 55-60 (2003).
  - [10] R . Shaw R , The D ripping faucet as a m odel of a chaotic system , (Aerial P ress, Santa C ruz 1984).
  - [11] N . Fuchikam i, S . Ishioka, and K . K iyono, J. Phys. Soc. Jpn., 68 (4) 1185-1196 (1999).
  - [12] P . C oullet, L . M ahadevan, and C . R iera C ., Prog. Theor. Phys. Suppl., No. 139 (2000)